MOLECULAR DYNAMICS SIMULATIONS OF HEAT TRANSFER ISSUES IN CARBON NANOTUBES

S. Maruyama, Y. Igarashi, Y. Taniguchi and Y. Shibuta

Department of Mechanical Engineering, University of Tokyo, 7-3-1 Hongo, Bunkyo-ku, Tokyo 113-8656, JAPAN

ABSTRACT

Several heat transfer problems related to single-walled carbon nanotubes (SWNTs) are considered through molecular dynamics (MD) simulations. MD simulations of thermal conductivity along a nanotube, isotope effect in longitudinal thermal conductivity, and thermal boundary resistance in a junction of nanotubes are reviewed. Then, the heat transfer from an SWNT to various surrounding materials is simulated by MD simulations. Heat transfer between nanotubes in a bundle of nanotubes and between a nanotube and water are considered. The heat transfer rate can be well expressed by employing the thermal boundary resistance (TBR). The value of thermal boundary resistance is compared for nanotube-junction, bundle, and water-nanotubes cases.

INTRODUCTION

Single-walled carbon nanotubes (SWNTs) [1] have remarkable electrical, optical, mechanical, and thermal properties [2, 3]. In this paper, the thermal properties and heat transfer issues are considered from molecular dynamics (MD) simulations.

We have been studying the heat conduction along a SWNT by MD method [4-7] with the simplified form [8] of Tersoff-Brenner bond order potential [9]. Our preliminary results showed that thermal conductivity was strongly dependent on the nanotube length for realistic length scale for device applications [5, 6]. Furthermore, we have reported the direct calculation of phonon dispersion relations and phonon density of states from molecular dynamics trajectories [5, 6]. For more practical situations, the isotope effect on thermal conductivity and thermal boundary resistance in a nanotube junction were discussed from MD simulation results [7].

In addition to the thermal conductivity along a SWNT, heat transfer from a nanotube to the surrounding material is quite important for the practical applications using carbon nanotubes as electrical devices and composite materials [7]. In this paper, in addition to a review of simulations of thermal conductivity, isotope effect, and thermal boundary resistance of a junction, the heat transfer from an SWNT to various surrounding materials is simulated by MD simulations. Heat transfer between nanotubes in a bundle of nanotubes and between water and a nanotube are considered. The heat transfer rate can be well expressed by the thermal boundary resistance (TBR). The value of thermal boundary resistance is compared for nanotube-junction, bundle, and water-nanotubes cases.

SIMULATION TECHNIQUE

The Brenner potential [9] with the simplified form [8] is employed as the potential function between carbon and carbon within a nanotube. This potential can describe variety of small hydrocarbons, graphite and diamond lattices. The basic formulation of the potential is based on the covalent-bonding treatment developed by Tersoff [10]. The total potential energy of the system E_b is expressed as the sum of the bonding energy of each bond between carbon atoms *i* and *j*.

$$E_b = \sum_i \sum_{j(i<j)} \left[V_R(r_{ij}) - B_{ij}^* V_A(r_{ij}) \right], \tag{1}$$

where $V_R(r)$ and $V_A(r)$ are repulsive and attractive force terms, respectively. The Morse type form with a cut-off function $f(r)$ expresses these terms.

$$V_R = f(r) \frac{D_e}{S-1} \exp\left\{ -\beta\sqrt{2S}(r - R_e) \right\} \tag{2}$$

$$V_A = f(r) \frac{D_e S}{S-1} \exp\left\{ -\beta\sqrt{2/S}(r - R_e) \right\} \tag{3}$$

$$f(r) = \begin{cases} 1 & (r < R_1) \\ \frac{1}{2}\left(1 + \cos\frac{r - R_1}{R_2 - R_1}\pi \right) & (R_1 < r < R_2) \\ 0 & (r > R_2) \end{cases} \tag{4}$$

The effect of the bonding condition of each atoms is taken into account through B_{ij}^* term which is the function of angle θ_{ijk} between bonds *i-j* and *i-k*.

$$B_{ij}^* = \frac{B_{ij} + B_{ji}}{2}, B_{ij} = \left(1 + \sum_{k(\neq i,j)} G_c(\theta_{ijk}) f(r_{ik}) \right)^{-\delta}, \tag{5}$$

where

$$G_c(\theta) = a_o \left(1 + \frac{c_o^2}{d_o^2} - \frac{c_o^2}{d_o^2 + (1 + \cos\theta)^2} \right) \tag{6}$$

Constants are shown in Table 1. Here, we have employed the parameter set II (table 2 in [9]), which better reproduces the force constant.

Here, we have ignored [8] the term for the conjugate bond from original expressions of Brenner. The velocity Verlet method was adopted to integrate the equation of motion with the time step of 0.5 fs.

HEAT CONDUCTIVITY OF SWNTs

In our previous reports [4-7], thermal conductivity was calculated from the measured temperature gradient and the heat flux obtained by the energy budgets of phantom molecules. After obtaining the average temperature of about 300 K or 100 K with the auxiliary velocity scaling control, typically 1 ns simulations were performed for the equilibration with only phantom temperature control. Then, typically 2 ns calculation was used for the measurement of temperature

Table 1. Parameters for Brenner potential

D_e [eV]	R_e [Å]	S	R_1 [Å]	R_2 [Å]
6.0	1.39	1.22	1.7	2.0
β [Å^{-1}]	δ	a_0	c_0	d_0
2.1	0.5	0.00020813	330	3.5

distribution, with 20 K temperature difference. With energy budgets of controlling phantom molecules, the heat flux along the tube can be simply calculated. Combined with the temperature gradient, the thermal conductivity λ can be calculated through Fourier's equation,

$$q = -\lambda \frac{\partial T}{\partial z} \tag{7}$$

As the definition of cross-sectional area *A* of a nanotube, 2 different definitions are possible. One is to use the area of a hexagon dividing a bundle of SWNTs [4, 7]: $A = 2\sqrt{3}(d/2 + b/2)^2$, where *b* is van der Waals thickness 0.34 nm. On the other hand, ring of van der Waals thickness: πbd can also be a proper definition [5, 6]. The former definition is appropriate for the calculation of amount of heat which can be conducted by nanotubes packed in a limited cross-sectional area. This definition is also essential for the measurement of the enhancement of thermal conductivity with a double-walled carbon nanotube (DWNT) or peapod. Here, DWNT is made of 2 concentric SWNTs and peapod is an SWNT filled with fullerene inside. On the other hand, the latter definition is suited for comparison of SWNTs with different diameters [5, 6], because the thermal conductivity should be primarily proportional to the circumferential length of a nanotube.

The calculated thermal conductivity for a finite length nanotube was not as high as the previously reported result that it might be as high as 6600 W/mK at 300 K [11]. However, the thermal conductivity is much higher than high-thermal conductivity metals. The dependence of the thermal conductivity on the nanotube length [6] is summarized in Fig. 1. The thermal conductivity was diverging with the power-law characteristics with nanotube length [5, 6] at least up to the 0.4 μm long nanotube for (5, 5). This divergence is most dominant for the smallest diameter nanotube (5, 5). This very striking behavior of thermal conductivity is similar to the one-dimensional model calculations of thermal conductivity [12, 13] where the divergence of λ with the power of 0.35 or 0.4 is discussed. It seems that the one-dimensional feature of heat conduction is really possible with the real material: the small diameter carbon nanotube. The thermal conductivity may converge when the tube length is much longer than the mean free path of energy carrying phonon. However, the thermal conductivity of about 600 W/mK for about 0.4 μm tube is still steadily increasing with the exponent of 0.27 in Fig. 1.

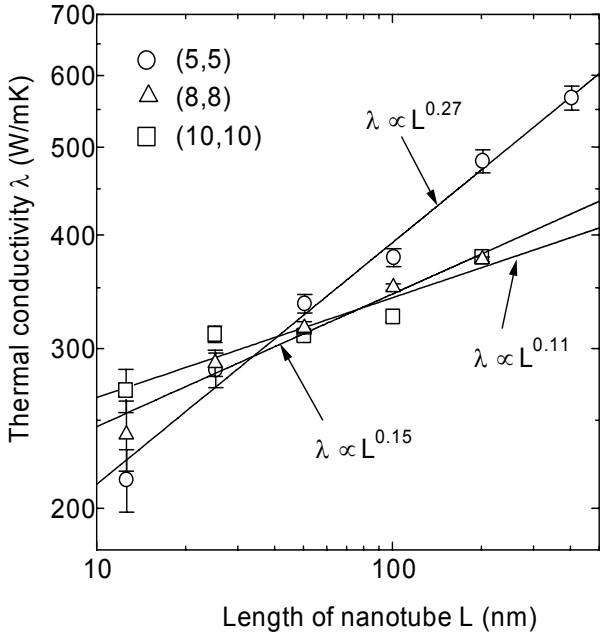

Fig. 1 Dependence of thermal conductivity on length of nanotubes for 300 K [6].

EFFECT OF ISOTOPE FOR HEAT CONDUCTION

Thermal conductivity of nanotube with randomly distributed ^{13}C with various ratios was calculated in our previous paper [7]. A preliminary result is shown in Fig. 2. Here, (5, 5) nanotube with about 50 nm was tested. The dependency of thermal conductivity on isotope ratio was well explained with the following equation as the fit lines in Fig. 2.

$$\lambda = \sqrt{\frac{12}{12(1-\beta)+13\beta}} \cdot \frac{\lambda_{pureC^{12}}}{C_1 \cdot \beta(1-\beta)+1}, \tag{8}$$

where β is the ratio of ^{13}C, $\lambda_{pureC^{12}}$ is the thermal conductivity for pure ^{12}C, C_1 is the fitting parameter. It is also noted that the thermal conductivity at 100 K is not

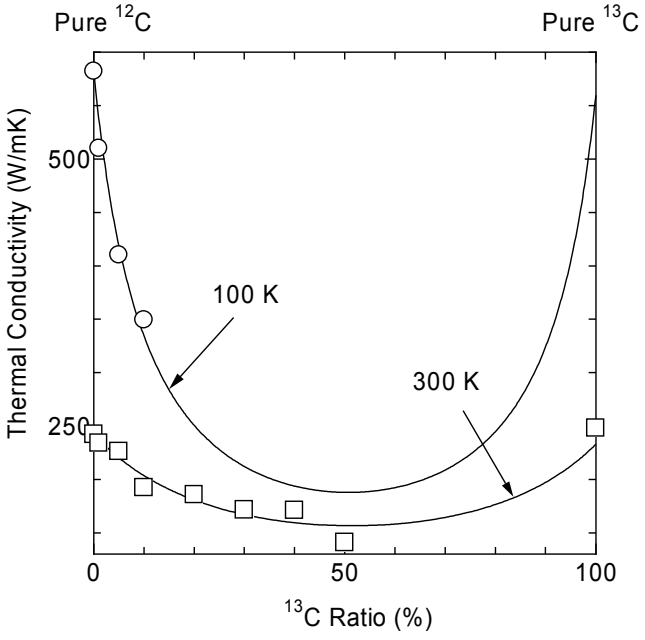

Fig. 2 Effect of ^{13}C isotope on thermal conductivity of SWNT [7].

realistic in Fig. 2 because the classical simulation cannot reproduce the correct change of heat capacity at low temperature [6]. The mechanism of the decrease of thermal conductivity with isotopes should be further discussed.

THERMAL RESISTANCE AT A SWNT JUNCTION

One example of the interesting feature is the thermal boundary resistance at the junction of nanotubes with different chiralities. The simulation system is shown in Fig. 3. In this case a (12, 0) zigzag nanotube in the left-hand side and a (6, 6) armchair nanotube were smoothly connected using 5-membered and 7-membered rings at the junction. By applying different temperatures at each end, temperature distribution was measured as in Fig. 4. The temperature jump at the junction is clearly observed. This temperature jump can be modeled by assuming that there is a virtual boundary between two nanotubes with different structures. The thermal boundary resistance at this virtual interface should be defined as follows.

$$R \equiv \frac{1}{h} = \frac{A\Delta T}{Q} \tag{9}$$

The thermal boundary resistance of the junction is calculated as 7.0×10^{-11} [m^2K/W] using the values in Table 2. Here, the cross-sectional area was defined as πbd.

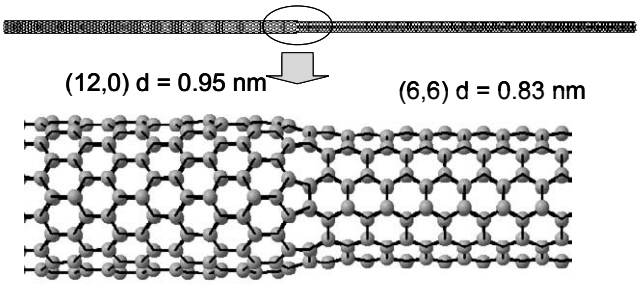

Fig. 3 Junction of two different SWNTs.

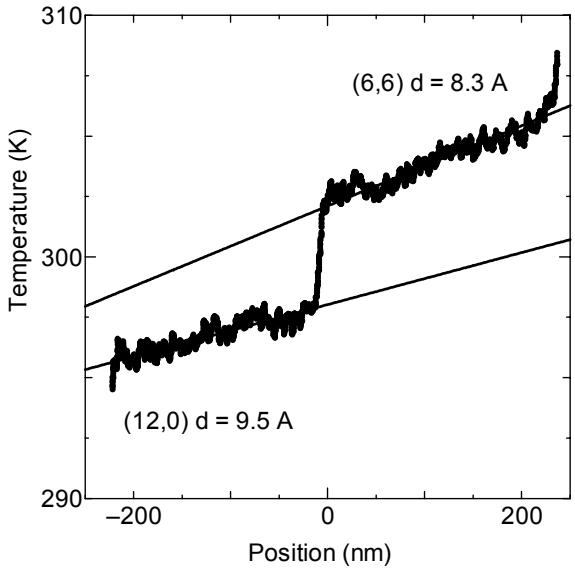

Fig. 4 Temperature jump at the junction by thermal boundary resistance.

Table 2 Parameters used for TBR calculation of junction

d [nm]	A [nm^2]	ΔT [K]	Q [W]
0.83194	0.889	4.05	5.16×10^{-8}

Table 3. Parameters for L-J potentials

	σ [nm]	ε [meV]
Carbon-Carbon	0.337	2.400
Carbon-Water	0.319	0.674

THERMAL BOUNDARY RESISTANCE OF SWNT BUNDLE

Simulation Techniques

In addition to Brenner potential between carbon atoms within an SWNT, van der Waals force between carbon atoms in different SWNTs was expressed as 12-6 Lennard-Jones potential with parameters in Table 3.

As the initial condition, 7 SWNTs whose length were 5 nm were located in the 5×6×6 [nm] simulation cell as in Fig. 5. The geometrical structure of SWNT was armchair type (5, 5) with diameter 0.693 nm. From the start of the calculation, the whole system was kept at 300K for 100ps. Then, the temperature of only the central SWNT was suddenly increased to 1000K using the velocity scaling method for 10 ps. After this, all temperature control were stopped.

Results and Discussion

Fig. 6 shows temperature change of hot (central) tube and cold (surrounding) tubes. The heat transfer from central tube to surrounding tubes is clearly observed in Fig. 6. In order to examine this heat transfer, temperature difference of central and surrounding tubes is drawn in Fig. 7. The monotonic decay of temperature difference in Fig. 7 was well

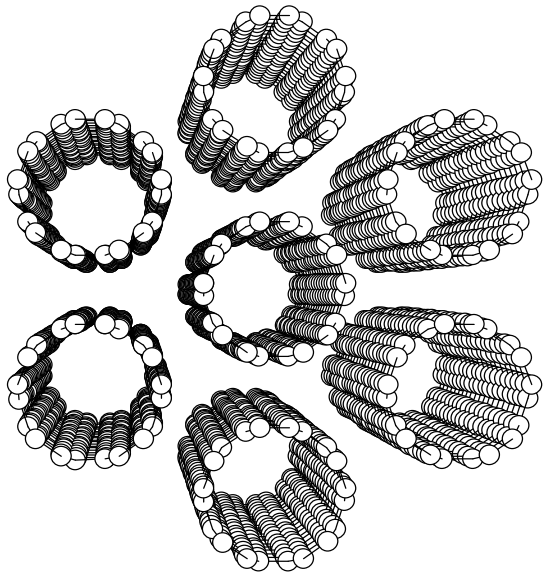

Fig. 5 Initial condition of SWNT bundle simulation. The central tube is suddenly heated up to 1000K.

approximated by an exponential function in Eq. (10)

$$T_{hot} - T_{cold} = T_0 \exp\left(-\frac{t}{\tau}\right) \tag{10}$$

where

$$T_0 = 875\,[K], \quad \tau = 29.7\,[ps]$$

If an SWNT is considered to be a solid material and heat transfer from the central tube to surrounding tubes is expressed by heat transfer coefficient or thermal boundary resistance (inverse dimension of heat transfer coefficient), the lump method in Eq. (11) can be adopted, since the characteristic length of an SWNT is extremely small. The diameter of SWNT is about 1 nm and the Biot number in Eq. (12) becomes very small.

$$T_{hot} - T_{cold} = T_0 \exp\left(\frac{-St}{R\rho cV}\right) \tag{11}$$

$$Bi = \frac{hL}{\lambda} \tag{12}$$

The excellent agreement to an exponential fit by Eq. (10) in Fig. 7 is understood by this concept. Comparing Eq. (10) with Eq. (11), the thermal boundary resistance R was estimated. By using values in Table 4, the thermal boundary resistance between SWNTs in a bundle was about 6.46×10^{-8} [m^2K/W].

The thermal conductivity of SWNT was estimated to be about 1000 W/mK in axial direction. One of the characteristics of heat transfer of SWNT is the strong anisotropy. By using the thermal resistance, axial and radial heat conduction are compared as follows.

For an SWNT with length L, thermal resistance of axial direction is expressed as

$$R_{axial} = \frac{L}{A\lambda} \tag{13}$$

where A is the cross-sectional area. On the other hand, the thermal resistance in radial direction is represented as

$$R_{radial} = \frac{1}{Sh} \tag{14}$$

where S is the cylindrical surface area. The length of an SWNT with which these thermal resistances are equal, can be the characteristic length of the thermal boundary resistance. Here, we define the characteristic length of TBR (L_{TBR}) as

$$\frac{L_{TBR}}{\left(\frac{\pi}{4}d^2\right)\lambda} = \frac{1}{(\pi d L_{TBR})h}$$

$$L_{TBR} \equiv \frac{1}{2}\sqrt{\frac{\lambda d}{h}} = \frac{\sqrt{R\lambda d}}{2} \tag{15}$$

By using Eq. (15), the characteristic length of TBR for the SWNT bundle is calculated as 0.105 μm as in Table 4. In other words, when the length of SWNT is 0.105 μm, the thermal resistance of axial direction and that of radial direction are similar. Suppose you are using an SWNT as a promotor of heat conduction as a composite material, thermal boundary resistance determines the performance for a shorter nanotube than L_{TBR}.

THERMAL BOUNDARY RESISTANCE BETWEEN SWNT AND WATER

Simulation Techniques

The Brenner potential was used between carbon and carbon. Water molecules were expressed by SPC/E potential [14]. SPC/E potential is expressed as the

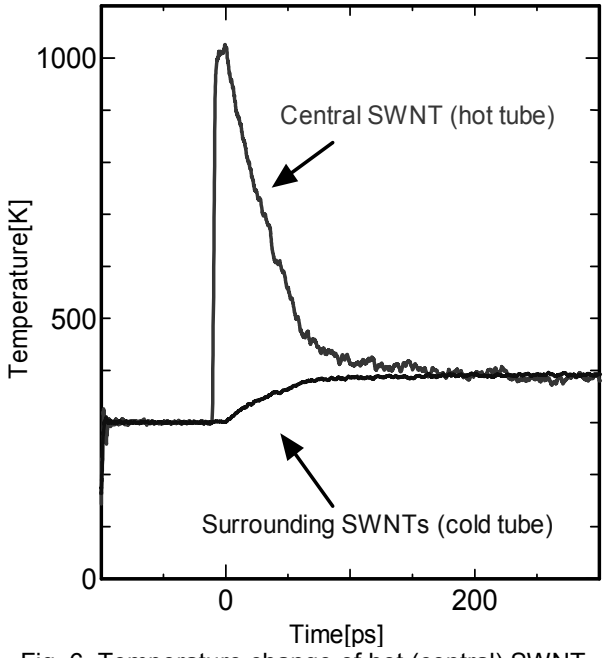

Fig. 6 Temperature change of hot (central) SWNT and cold (surrounding) SWNTs.

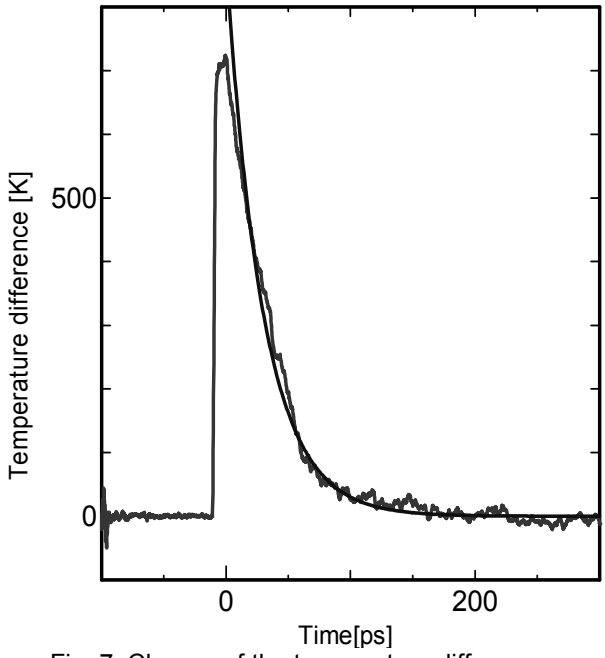

Fig. 7 Change of the temperature difference.

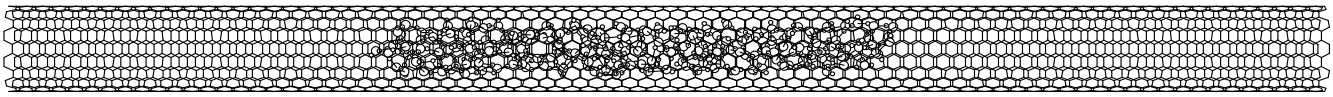

Fig. 8 Initial condition of the SWNT and Water molecules simulation.

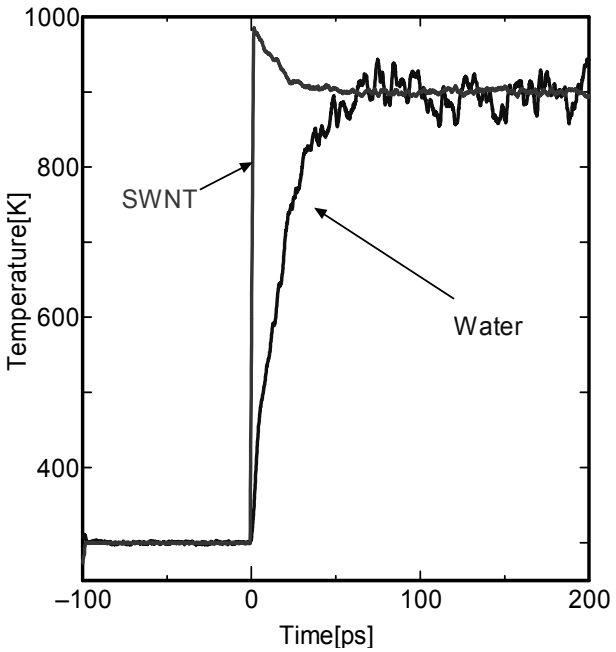

Fig. 9 Temperature change of SWNT and Water.

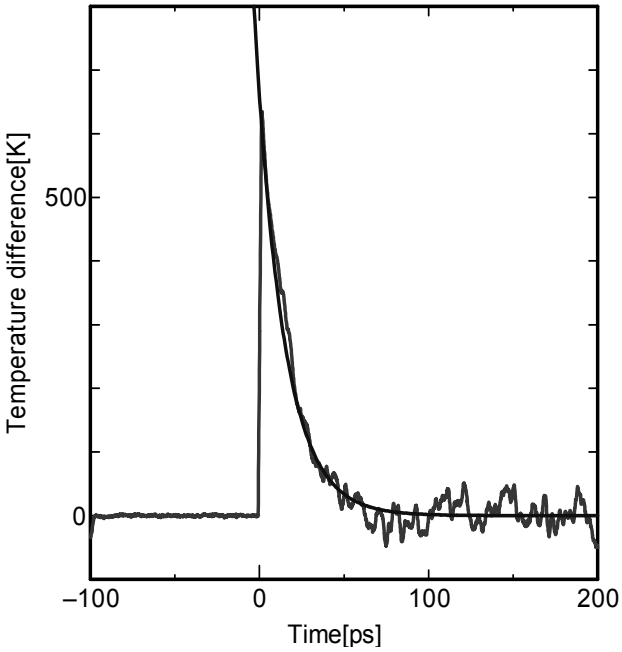

Fig. 10 Change of the temperature difference.

Table 4. The characteristic length of TBR

	S [nm^2]	ρV [kg]	C [J/kgK]	R [m^{2}K/W]	L_{TBR} [μm]
SWNT and SWNT	18	7.97×10^{-24}	1039	6.46×10^{-8}	0.105
SWNT and Water	28.8	5.74×10^{-24}	692	1.22×10^{-7}	0.204

superposition of Lennard-Jones function of oxygen-oxygen interaction and the electrostatic potential by charges on oxygen and hydrogen as follows.

$$\phi_{12} = 4\varepsilon_{OO}\left[\left(\frac{\sigma_{OO}}{R_{12}}\right)^{12} - \left(\frac{\sigma_{OO}}{R_{12}}\right)^{6}\right] + \sum_i \sum_j \frac{q_i q_j e^2}{4\pi\varepsilon_0 r_{ij}} \qquad (16)$$

where R_{12} represents the distance of oxygen atoms, and σ_{OO} and ε_{OO} are Lennard-Jones parameters. The Coulombic interaction is the sum of 16 pairs of point charges.

The potential function between water molecules and carbon atoms are represented by Lennard-Jones function (with parameters in Table 3) and the quadropole interaction term [15].

One (10, 10) SWNT with length 20.118 nm and 192 water molecules inside it were prepared in the 20.118×10×10 nm fully-periodic simulation cell as in Fig. 8.

At the initial stage of simulation, water molecules and the SWNT were equilibrated at temperature of 300 K. Then, only the temperature of the SWNT was suddenly heated up to 1000K. And all temperature control was stopped.

Results and Discussion

Fig. 9 shows the temperature change of the SWNT and water molecules. The heat transfer from hot SWNT to water is observed. Fig. 10 shows temperature difference. Again an exponential fit in Eq. (10) is possible with following parameters.

$$T_0 = 659\,[K], \quad \tau = 16.8\,[ps]$$

The thermal boundary resistance is estimated to be 1.22×10^{-7} [m^{2}K/W] using the lump method similarly to the case of SWNT bundle simulation.

The characteristic length of TBR between the SWNT and water molecules is also calculated using Eq. (15) as 0.204μm.

CONCLUSIONS

The thermal boundary resistances related to an SWNT are calculated by molecular dynamics method.

When SWNTs which have different chiralities are joined, the thermal boundary resistance of the junction are estimated to be 7.0×10^{-11} [m^{2}K/W]. On the other hand, the thermal boundary resistance between the SWNTs in a bundle or between the SWNT and water was estimated to be 6.46×10^{-8} [m^{2}K/W] or 1.22×10^{-7} [m^{2}K/W], respectively.

In order to compare these values with SWNT's axial thermal conductivity, we define the characteristic length scale of thermal boundary resistance. The values are calculated as 0.105 μm in the SWNT bundle case, and 0.204 μm in the SWNT and water molecules case, respectively.

NOMENCLATURE

A	cross section area of a SWNT [m^2]
Bi	Biot number
c	specific heat [J/kg K]
e	charge of electron [J]
h	heat transfer coefficient [W/m^2K]
L	length of nanotube [m]
q	heat flux per area [W/m^2]
Q	heat flux [W]
R	thermal boundary resistance [m^2K/W]
S	surface area [m^2]
T	temperature [K]
V	volume [m^3]
V_A	Attractive term of Brenner potential [J]
V_R	Repulsive term of Brenner potential [J]
ε	L-J potential parameter [J]
ε_0	dielectric constant [F/m]
λ	thermal conductivity [W/mK]
ρ	density [kg/m^3]
σ	L-J potential parameter [Å]
τ	fitting parameter [s]

Subscripts

axial	axial direction
cold	cold (surrounding) SWNT
hot	hot (central) SWNT
radial	radial direction

REFERENCES

1. S. Iijima and T. Ichihashi, Single-Shell Carbon Nanotubes of 1-nm Diameter, Nature, vol. 363 (1993), pp. 603-605.
2. M. S. Dresselhaus, G. Dresselhaus and P. C. Eklund, Science of Fullerenes and Carbon Nanotubes, Academic Press, New York, 1996.
3. R. Saito, G. Dresselhaus and M. S. Dresselhaus, Physical Properties of Carbon Nanotubes, Imperial College Press, London, 1998.
4. S. Maruyama and S.-H. Choi, Molecular Dynamics of Heat Conduction through Carbon Nanotube, Therm. Sci. Eng., vol. 9 (2001), pp. 17-24.
5. S. Maruyama, A Molecular Dynamics Simulation of Heat Conduction in Finite Length SWNTs, Physica B, vol. 323 (2002), pp. 272-274.
6. S. Maruyama, A Molecular Dynamics Simulation of Heat Conduction of a Finite Length Single-Walled Carbon Nanotube, Micro. Thermophys. Eng., vol. 7 (2003), pp. 41-50. x
7. S. Maruyama, Y. Miyauchi and Y. Taniguchi, Effect of Carbon Isotope Abundance on Thermal Conductivity and Raman Scattering of Single-Walled Carbon Nanotubes, International Symposium on Micro-Mechanical Engineering, Tsukuba, (2003) in press.
8. Y. Yamaguchi and S. Maruyama, A Molecular Dynamics Simulation of the Fullerene Formation Process, Chem. Phys. Lett., vol. 286 (1998), pp. 336-342.
9. D. W. Brenner, Empirical Potential for Hydrocarbons for Use in Simulating the Chemical Vapor Deposition of Diamond Films, Phys. Rev. B, vol. 42 (1990), pp. 9458-9471.
10. J. Tersoff, New empirical model for the structural properties of silicon, Phys. Rev. Lett., vol. 56, (1986), pp. 632-635.
11. S. Berber, Y.-K. Kwon and D. Tomanek, Unusually High Thermal Conductivity of Carbon Nanotubes, Phys. Rev. Lett., vol. 84 (2000), pp. 4613-4616.
12. R. Livi and S. Lepri, Heat in One Dimension, Nature, vol. 421 (2003), pp. 327-327.
13. S. Lepri, Memory Effects and Heat Transport in One-Dimensional Insulators, *Eur. Phys. J. B*, vol. 18, (2000), pp. 441-446.
14. H.J.C. Berendsen, J.R. Grigera and T.P. Straatsma, The missing term in effective pair potentials, *J. Phys. Chem*., 91-24 (1987), pp. 6269-6271.
15. J.H. Walther, R. Jaffe, T. Halicioglu and P. Koumoutsakos, Carbon Nanotubes in Water: Structural Characteristics and Energetics, *J. Phys. Chem. B*, 105 (2001), pp. 9980-9987.
16. S. Maruyama, Molecular Dynamics Method for Microscale Heat Transfer, Advances in Numerical Heat Transfer, vol. 2 (2000), pp. 189-226.